# Formation of large micellar aggregates before equilibrium in diluted solutions

J. N. B. de Moraes* and W. Figueiredo†

*Departamento de Física, Universidade Federal de Santa Catarina, 88040-900, Florianópolis, Santa Catarina, Brazil*

(Received 3 February 2013; revised manuscript received 19 March 2013; published 20 June 2013)

We study the formation of premicelles for different values of the concentration of amphiphile molecules in water. Our model consists of a square lattice with water molecules occupying one cell of the lattice while the amphiphilic molecules, represented by chains of five interconnected sites, occupy five cells of the lattice. We perform Monte Carlo simulations in the *NVT* ensemble, for a fixed temperature and different concentration of amphiphiles, ranging from below to above the critical micelle concentration. We start our simulations from a monomeric state and follow in time all the aggregates sizes until the equilibrium state is reached. We pay particular attention to two aggregate sizes, one related to the minimum and the other to the maximum of the aggregate-size distribution curve obtained at equilibrium. We show that these aggregates evolve in time exhibiting a maximum concentration well before the equilibrium state, revealing the formation of premicelles. The times to reach these maximum concentrations decrease exponentially with the total concentration of the system.

DOI: 10.1103/PhysRevE.87.062315 PACS number(s): 82.70.Uv, 82.20.Rp, 47.57.jb, 02.70.Uu

## I. INTRODUCTION

A very old and interesting problem in the physics of complex systems is the self-assembly of amphiphilic molecules in aqueous solution. These molecules are chemical compounds formed by hydrophilic and hydrophobic parts that are strongly coupled to each other. While the hydrophilic head group likes to be in contact with the water molecules, the hydrophobic carbonic tail avoids a direct contact with water [1,2]. Depending on the concentration and temperature, when dispersed in water, they self-assemble into aggregates of different sizes and shapes like micelles, vesicles, and bilayers [3–5]. The spectrum of application of these special molecules is very wide, ranging from industry [6], medicine [7], engineering, environmental science, and technology [8–10].

An important parameter regarding the aqueous solutions of amphiphiles is the so-called critical micelle concentration (CMC). Above this concentration, the amphiphiles form aggregates of different sizes and forms. For most amphiphiles, the interior of the aggregates contains hydrophobic hydrocarbon chains, while the hydrophilic head segments remain at the surface in direct contact with the water [4]. Wennerstrom and Lindman [11] defined the formation of micelles, observing the behavior of the aggregate-size distribution curve. When the concentration of isolated amphiphiles becomes constant with increasing values of the total concentration of solution, and the aggregate-size distribution curve presents a minimum and a maximum, we are in a micellized state. Otherwise, below the CMC, the curve of the aggregation number is a monotonic decreasing function of the aggregate size, and we have a nonmicellar state. For a fixed total concentration of amphiphiles, the state of the system can be changed by temperature variations [12]. In this paper, we are considering only nonionic amphiphiles, because in the case of ionic ones the free monomer concentration decays with increasing total surfactant concentration, as has been shown in theoretical [13,14] and experimental [15] studies. For a system in the micellized state, we can calculate the difference $\Delta$ between the concentrations at the maximum and at the minimum of the aggregate-size distribution curve as a function of temperature. The parameter $\Delta$ goes to zero at a given temperature $T_M$, at which the system becomes nonmicellized. Close to $T_M$, the parameter $\Delta$ decreases linearly with increasing temperature in two dimensions [12], while it decreases quadratically in three dimensions [16,17]. The CMC in some experimental studies exhibits a minimum as a function of temperature [18,19]. This nonmonotonic behavior has been confirmed by Monte Carlo simulations performed in the grand canonical ensemble [20,21]. In this work, we defined the CMC for a fixed temperature, when the concentration of free amphiphiles becomes constant as a function of the total concentration, which represents the concentration of amphiphiles to form micelles in solution. We also checked the value of the parameter $\Delta$, which must be different from zero in a micellized state. There are other definitions of CMC, such as, for instance, that employed by Cheong and Panagiotopoulos [22] based on the point of inflection of the osmotic pressure curve versus concentration.

It is well known that the appearance of large aggregates occurs even for concentrations well below the CMC, a phenomenon called premicellar aggregation. There are many different experimental [23–29] studies and theoretical predictions [30–34] related to premicellar aggregation in diluted solutions. Using a simple two-state model, where only monomers and aggregates of the same size are possible, Hadgiivanova and Diamant [31] determined the metastable states of the system for concentrations below the CMC. They extended their results to include polydispersity [32] and calculated the lifetime of the metastable aggregates. Based on a free-energy formalism [33], a kinetic of surfactant micellization is considered for concentrations above the CMC. Three different stages are identified: formation of critical nuclei, intermediate aggregates and equilibrium, with three different time scales. It is a further step on the theoretical studies performed by Aniansson and coworkers [35,36], relative to the dynamics of micellar aggregation, where two time scales were considered. Recently [34], properties of premicelles were investigated for concentrations below and

*joaquim@fisica.ufsc.br
†wagner@fisica.ufsc.br

 

above CMC through molecular dynamics simulations. They showed that the premicelles exhibited a great variety of shapes, ranging from elongated chain-like cores to the more traditional micelle-like structures.

In the present study, we consider the multisite chain model proposed by Larson [37,38], where the amphiphilic molecules are represented by interconnected sites on the lattice. Our system presents a large polydispersity due to the short size of the amphiphilic molecules, and we investigate the time evolution of aggregates toward equilibrium for concentrations below and above the CMC. We employ in these studies, lattice Monte Carlo simulations, which have been extensively used to describe the micellar systems [37–48]. A real difficulty with Monte Carlo simulations is to relate the time intervals with the real time. While in molecular dynamics during a single time step we perform a local update, in Monte Carlo simulations, few time steps can represent large changes in the phase space of the system. In this sense, Monte Carlo simulations are useful because during a simulation we have the opportunity to visit the most representative states of the system, and the time arrow points in the same direction as the real time. We start our simulations from an initial state where the amphiphiles are free, which corresponds to very high temperatures, to the equilibrium state where aggregates of different sizes are formed. Particularly, we look at the times where the aggregates, which are the minimum ($m$) and the maximum ($M$) in the aggregate-size distribution curve at equilibrium, exhibit their highest values as a function of total concentration of the solution. These typical aggregates appear as premicellar aggregates just at the beginning of the experiments, corresponding to times several orders away from the equilibrium.

We have selected three regions of concentrations to observe these features. One below the CMC, another one just above the CMC, and yet another one far from the CMC. The most important case happens for concentrations below CMC, where large aggregates form at the beginning of the simulations. For instance, the aggregates ($m$) that correspond to the minimum of the aggregate-size distribution curve attain concentrations as large as the concentration of the free amphiphiles, just before they start to nucleate larger aggregates. The maximum concentration of the premicellar aggregates ($M$) occurs 20 times later than the ($m$) aggregates reached their maximum concentration. On the other hand, for concentrations close and far from the CMC, the aggregates ($m$) exhibit a maximum concentration that is larger than the concentration of the free amphiphiles; that is, the maximum concentration of ($m$) aggregates increase with the total concentration of the solution. We have also observed that the times to attain the maximum values of the concentration for the aggregates ($m$) and ($M$) decrease exponentially with the total concentration. In the next section, we describe the model and some details regarding our Monte Carlo simulations; in Sec. III, we present our results and discussions; and in Sec. IV, we present our conclusions.

## II. MODEL AND SIMULATIONS

Our model considers a square lattice with periodic boundary conditions, filled by single-site solvent molecules and by self-avoiding chains of connected sites representing the amphiphiles, to study the aggregation of amphiphiles in a dilute solution. The amphiphilic molecules are represented by five interconnected monomers, each monomer occupying a single cell of the lattice. They are represented by the formula $H_1T_4$, where the $H$ denotes the hydrophilic part of the molecule and $T$ its hydrophobic part, which avoids a direct contact with the solvent molecules. The remaining cells of the lattice are filled with water molecules, each one occupying a single cell. We consider only interactions between particles located on nearest-neighbor cells of the lattice. Our model is not sufficiently realistic to compare with experimental data; only qualitative comparisons are possible, because our hydrophobic chain is very short and our simulations are performed in two dimensions. In this case, we have some limitations, such as, for instance, high polydispersity, and a not so large difference between the concentrations of the most probable aggregate size and that of the minimum, as seen in the case of long chains. Despite these facts, our model displays some general trends that are observed in real surfactant solutions, such as, for example, the formation of premicelles, the well-defined critical micellar concentration, as well as the aggregate-size distribution curve at equilibrium with well-defined values of the extrema concentrations. However, we lose some information regarding the structure and size of aggregates when we perform simulations in two dimensions. Although we have considered only very short molecules in our simulations, problems can appear when we need to simulate a system with long amphiphiles in two dimensions, because the reptation movement can leave the system blocked in some states, and other types of movements are necessary to circumvent these situations. At the end of the Conclusions section, we show how, from simulations in two dimensions, we can get some information about the corresponding simulations in three dimensions. Simulations in two dimensions are faster than in three dimensions; however, they capture the essentials of the micellization process, as we can see in our earlier works [12,16].

We have chosen the following set of parameters for the interactions between particles on nearest-neighbor cells: $E_{HH} = \varepsilon$, $E_{HT} = \varepsilon$, $E_{HS} = -\varepsilon$, $E_{TS} = -E_{TT} = \varepsilon$, $\varepsilon > 0$, where the subscripts read $S$ for solvent molecules, $T$ for monomers in the hydrophobic tail, and $H$ for the hydrophilic heads. We have also considered an attractive interaction between two nearest-neighbor water molecules, that is, $E_{SS} = -\varepsilon$. We have also added an energy penalty $\epsilon$ to each bending of the polymer chain. This choice favors a more straight chain conformation and allows for the presence of larger aggregates. As we are interested in the time evolution of aggregates of different sizes, these figures for the energy parameters of very short chains is compatible with a high polydispersity in the equilibrium state. Our simulations are carried out in the canonical ($NVT$) ensemble, where volume $V$ and temperature $T$ are fixed, and we allow for different values of the number of amphiphiles $N$; that is, we simulate our system for different concentrations. The linear size of the square lattice is $L = 200$ and we have considered $N$ ranging from 90 (low concentration, $0.20 \times$ CMC) to 1200 (high concentration, $2.22 \times$ CMC) amphiphiles, and where each amphiphile occupies five linked cells of the lattice. We fix the temperature at the value $T = 2.2$, which is measured

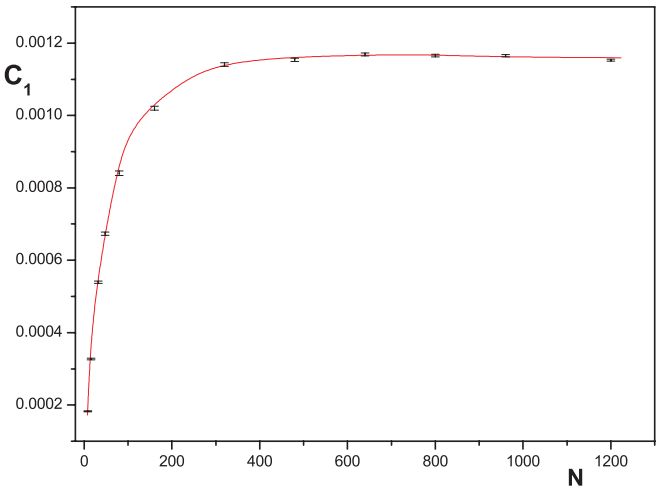


FIG. 1. (Color online) Free amphiphile concentration $C_1$ as a function of total concentration, expressed by the number $N$ of amphiphiles, for a square lattice of side $L = 200$, and temperature $T = 2.2$, measured in units of $\epsilon/k_B$. The CMC occurs around $N = 450$. The concentration $C$ is related to the number of molecules by $C = N/L^2$.

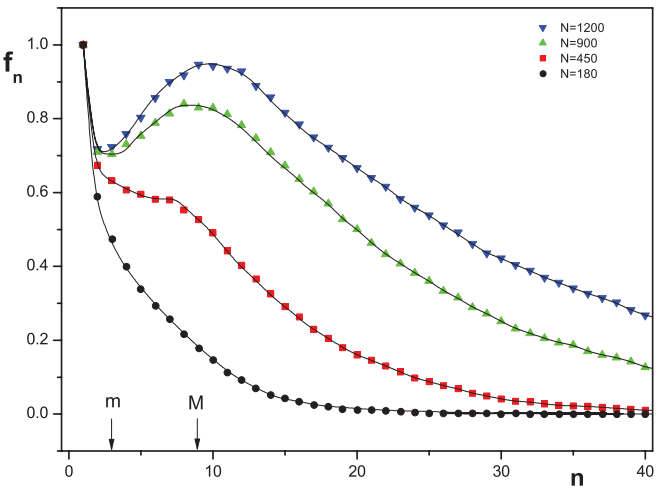


FIG. 2. (Color online) Relative aggregate-size equilibrium distribution curve as a function of the size of the aggregates for four different concentrations. The concentrations are $C = 0.0045$ for $N = 180$, $C = 0.01125$ for $N = 450$, $C = 0.0225$ for $N = 900$, and $C = 0.0300$ for $N = 1200$. Here, $L = 200$, $T = 2.2$, and $f_n = \frac{C_n}{C_1}$ is the concentration of the aggregates of size $n$ relative to the concentration of free amphiphiles. The lines serve to guide the eye. In this plot, $m = 3$ and $M = 9$ are the selected aggregate sizes for which we focus our attention during their evolution toward equilibrium.

in units of $\epsilon/k_B$, where $k_B$ is the Boltzmann constant. To start our simulations, we prepare our system in such a way that only free amphiphiles are present at the time $t = 0$. We get this by choosing very large values for the parameter $\epsilon$ and letting all the interactions be repulsive. After a few iterations, only isolated amphiphiles remain in the system. After that, we restore the original values of the interaction parameters to start the simulations. For the Monte Carlo simulations, we apply periodic boundary conditions and the changes in the state of the system are made according to the Metropolis prescription [49,50]. At each Monte Carlo step (MCs) we visit all the amphiphiles molecules and we attempt to move each one through the usual reptation movement, which is the basic type of movement in the Larson lattice model. For $N = 1200$, after $2 \times 10^5$ MCs the system reaches the thermal equilibrium, which is confirmed by the time evolution of the energy and the mean aggregate size [43]. We have seen that the usual criterion based on the stabilization of energy is not always sufficient to assure the thermodynamical equilibrium. It is necessary to monitor the time evolution of all the aggregate sizes to predict the correct equilibrium state. When we speak about time in this paper, in reality we are always referring to Monte Carlo steps. In our previous works [43,51], the time to attain the equilibrium state is four times longer than that required for the total energy to become constant. Then, the total number of steps we use in the present work, $3 \times 10^5$ MCs, is sufficient to describe the evolution toward equilibrium states for all the concentrations considered in this work. In order to get good statistics, we have considered averages over typically $10^3$ samples, obtained from independently prepared initial random samples. We compute at each instant of time the number density of aggregates of size $n$ by the relation $C_n = n \times N_n/L^2$, where $N_n$ is the number of aggregates containing $n$ amphiphiles. The total concentration is given by $C = \sum_{n=1}^{\infty} C_n$. In some plots we use the relative concentration $f_n$, which is defined by $f_n = \frac{C_n}{C_1}$ .

## III. RESULTS AND DISCUSSIONS

We show in Fig. 1 the concentration of isolated amphiphiles as a function of the total concentration for $T = 2.2$. We define the CMC as the lower value of $C$ for which the concentration of isolated amphiphiles becomes constant. Figure 2 exhibits the aggregate-size distribution curves at equilibrium for different concentrations and temperature $T = 2.2$. Due to the short size of the amphiphiles we get a solution with high polydispersity. We note that the maximum and minimum appear only for values of $N$ larger than 450. The relative concentration at the maximum increases with the total concentration, and the aggregation number at the maximum, which represents the typical micellar aggregate, increases slightly with the total concentration. For values of $N$ less than 450, the aggregate-size distribution curve is a monotonically decreasing function of the $n$, the size of the aggregates. In this region of low concentration

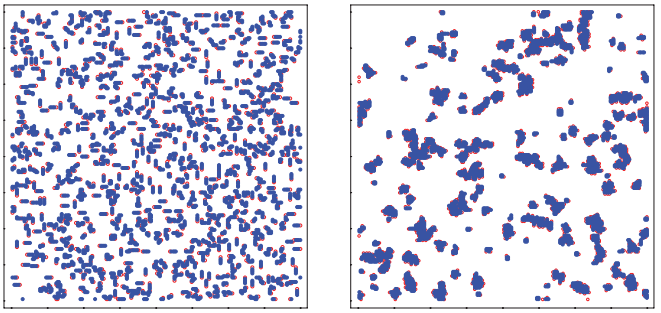


FIG. 3. (Color online) Snapshots of the spatial distribution of amphiphiles at $t = 0$ (a) and at $t = 3 \times 10^5$ MCs (b), when the system reached equilibrium. We have $L = 200$, $N = 900$ molecules ($C = 0.0225$) above the CMC, and $T = 2.2$.

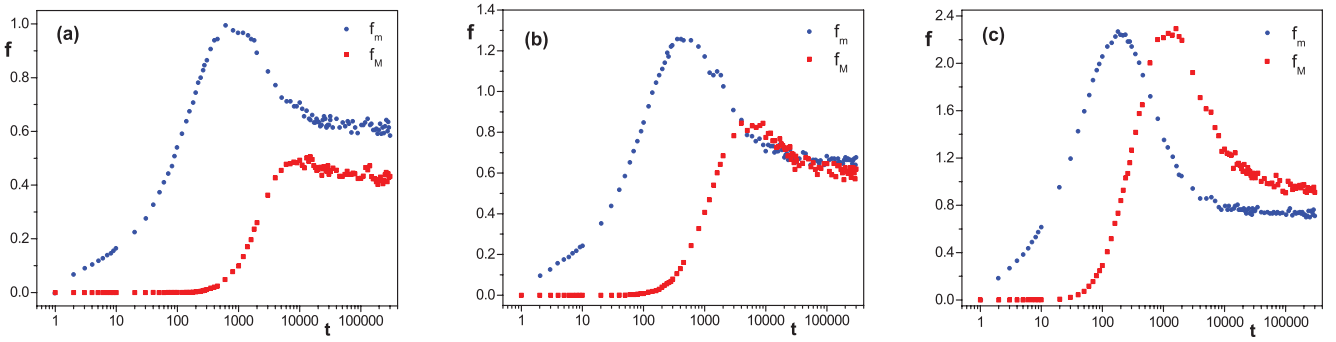


FIG. 4. (Color online) Time evolution of the relative concentration of the aggregates of sizes $n = 3$ and $n = 9$ for three different concentrations: ($a$) $C = 0.0090$ for $N = 360$, below the CMC, ($b$) $C = 0.0135$ for $N = 540$, just above the CMC, and ($c$) $C = 0.0300$ for $N = 1200$, well above the CMC. Here, we have $L = 200$ and $T = 2.2$. In these figures, we have $f_m = C_3/C_1$, $f_M = C_9/C_1$, and $t$ is measured in $MCs$.

of amphiphiles, we do not see a typical micellar aggregate, although they appear as premicelles at the early times of the evolution toward equilibrium, as we will see next. We see in Fig. 3 the spatial distribution of amphiphiles at $t = 0$ and at $t = 3 \times 10^5$, where equilibrium was already attained, for $N = 900$ molecules, above the CMC, and $T = 2.2$. As to be expected for short-size amphiphiles, the aggregates present a variety of shapes as pointed out by LeBard *et al.* [34]. We now turn our attention to the time evolution of aggregates. Figure 4 displays the behavior of the concentration as a function of time, for the aggregate sizes at the maximum, $n = 9$, and at the minimum, $n = 3$, observed in the aggregate-size distribution curves above the CMC ($N > 450$). We have plotted the time axis in a logarithmic scale and we also omitted the error bars for a better visualization of the time evolution of the relative concentration of the aggregates. We considered three different concentrations: curves ($a$) with $N = 360$, below the CMC, ($b$) with $N = 540$, just above the CMC, and ($c$) with $N = 1200$, well above the CMC, which corresponds to a concentration 2.67 × CMC. We note that even for $N = 360$, below the CMC, we observe the formation of premicellar aggregates. The relative concentration of the aggregates of sizes $n = 3$ and $n = 9$ increases with time reaching maximum values at times $t = 400$ MCs and $t = 10{,}000$ MCs, respectively. At the maximum we note that the concentration of the aggregates of size $n = 3$ is very close to the concentration of the isolated amphiphiles. The aggregates of size $n = 9$ start to appear just after the aggregates of size $n = 3$ reached its maximum concentration. Although we are below the CMC, the formation of these premicellar aggregates occurs at the expense of those aggregates of size around $n = 3$. The appearance of the maximum concentration for $n = 3$ occurs very early, approximately, $t_m = 1.3 \times 10^{-3}$ of the time to reach equilibrium, whereas the maximum concentration of premicelles of size $n = 9$ occurs at latter time, $t_M = 0.3 \times 10^{-1}$ of the equilibrium time. Looking at the concentration of the aggregates of size $n = 9$ in this figure, we note that after it reaches its maximum value at time $t_M$, it remains almost constant. Despite the entering and exiting of individual monomers from micelles, the aggregates of size $M$ become stable, because the total concentration is low, and the probability to form larger aggregates through fusion is very small. Figures 4(b) and 4(c) present the same trends as observed in Fig. 4(a); however the times to attain the maximum values of the concentration for the aggregates $n = 3$ and $n = 9$ decrease with the total concentration. We also observe that for concentrations larger than the CMC, the maximum concentration is always larger than the value of the concentration of isolated amphiphiles. The time $t_m$ for the aggregates of size $n = 3$ to reach their maximum corresponds to the nucleation time to form the critical nuclei [33]. Just after this instant, intermediate aggregates start to appear, whose maximum concentration occurs at time $t_M$ as we can see for the premicellar aggregate of size $n = 9$. Finally, the system relaxes toward equilibrium.

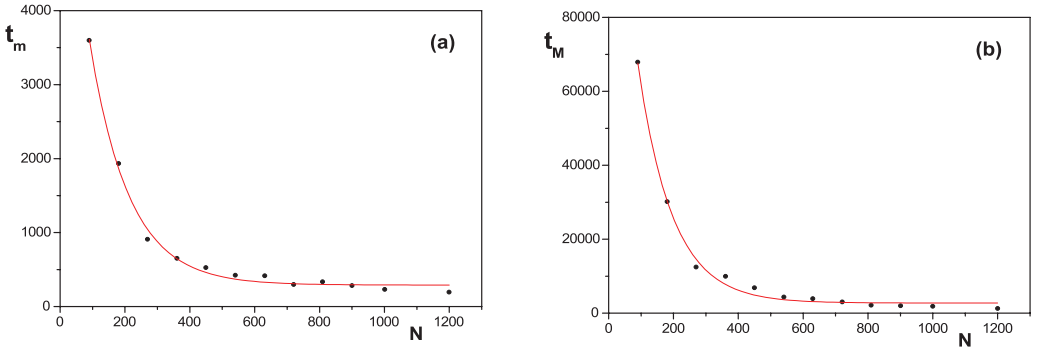


FIG. 5. (Color online) Times (a) $t_m$ and (b) $t_M$ at which the concentration of aggregates of sizes $n = 3$ and $n = 9$ reach their maximum, versus $N$. Times are measured in $MCs$ and the total number of molecules ($N$) is related to the concentration of the solution by $C = N/L^2$.

Figure 5 shows the times to reach the maximum concentration for the selected aggregates of sizes $n = 3$ and $n = 9$. We see that these times are exponentially decreasing functions of the total concentration. Both decays are expressed by the laws $t_m \approx \exp(-N/\tau_m)$ and $t_M \approx \exp(-N/\tau_M)$, where $N$ is the total number of amphiphiles, which is proportional to the total concentration of the solution. Interestingly, the typical concentrations $\tau_m$ and $\tau_M$ are very close to each other and are given by the values $\tau_m = 121 \pm 6$, and $\tau_M = 106 \pm 5$.

## IV. CONCLUSIONS

We have investigated the formation of premicelles through Monte Carlo simulations for a model of amphiphilic aggregation on a square lattice in the *NVT* ensemble. The system was prepared so that at the initial time all the amphiphiles are free in the solution. We follow the evolution in time of the aggregates until the equilibrium state is reached, for different concentrations of amphiphiles. For concentrations above the CMC, the aggregate size distribution curve, at equilibrium, exhibits a minimum and a maximum, which for the short amphiphiles we used, occur at $n = 3$ (minimum) and $n = 9$ (maximum). We studied the time evolution of these two special aggregates for various concentrations below and above the CMC. We have shown that the concentration of these aggregates exhibit a maximum at the early times of evolution. We identified three characteristic processes during the evolution to equilibrium: the first maximum at $t_m$ corresponds to the formation of the critical nuclei ($m$) aggregates, then until a next time $t_M$, when aggregates of size $n = 9$ present the highest concentration, we have the formation of intermediate aggregates, and finally, for times longer than $t_M$, the system relaxes toward equilibrium. An interesting feature is seen during simulations performed at small concentrations, below the CMC, where large aggregates form at the beginning of the simulations. Aggregates ($m$) that correspond to the minimum of the aggregate-size distribution curve reach concentrations as large as the concentration of the free amphiphiles, just before they start to nucleate the premicelles ($M$). The maximum concentration of the premicellar aggregates occurs 20 times later than the ($m$) aggregates reached their maximum. On the other hand, for concentrations close and far from the CMC, the aggregates ($m$) exhibit a maximum concentration that is larger than the concentration of the free amphiphiles. We have also seen that times $t_m$ and $t_M$ are exponentially decreasing functions of the total concentration. The scenario for the time evolution of the aggregates is in agreement with the thermodynamic calculations performed by Hadgiivanova *et al.* [33], where three time scales were employed to describe the evolution toward equilibrium of a solution of free amphiphilic molecules. Our Monte Carlo simulations are also in qualitative agreement with Molecular Dynamics simulations by LeBard *et al.* [34] for concentrations below and above the critical micellar concentration. In their work, they considered amphiphiles formed by 12 units, while in our case our amphiphiles are shorter, 5 units. They showed that the time ratio for the formation of full size micelles relative to premicelles is $72/1.3 \approx 55$, while in our calculations this ratio is given by $0.3 \times 10^{-1}/1.3 \times 10^{-3} \approx 23$, one half of that value, for concentration $C = 0.0090$, below the CMC. Although we have not performed simulations in three dimensions (3D), Fig. 4(a) helps us to understand what would happen in 3D. After the time $t_m$, large aggregates are mainly generated through the fusion process of small ones. The fusion time $T_f$ is proportional to the diffusion time of small aggregates, which in two dimensions (2D) can be written as $T_D(2\mathrm{D}) \approx l^2/(4D)$, where $l$ is a typical diffusion distance and $D$ is the diffusion coefficient. For low concentrations, in 3D we also can write that $T_D(3\mathrm{D}) \approx l^2/(6D)$, which gives $T_D(3\mathrm{D})/T_D(2\mathrm{D}) = 2/3$. As the fusion time also scales with total concentration(inverse of volume) we also expect that $T_f(2\mathrm{D})$ scales with $[T_f(3\mathrm{D})]^{3/2}$. Then, our ratio $t_M/t_m = 23$ in 2D should be $(23 * 2/3)^{3/2} = 60$ in 3D, a value very close to 55 observed by Le Bard *et al.* [34] in their 3D simulations of nonionic surfactants. This type of mapping between simulations in 2D and 3D can be used to estimate the time ratio ($t_M/t_m$) from the simple simulations in 2D to 3D for more realistic molecules. As a future work, we intend to perform simulations in 3D for our simple system in order to test the above reasonings. We also plan to make simulations in 2D and 3D for ionic surfactants for which we expect that the ratio between the times $t_M$ and $t_m$ are larger than for nonionic surfactants.

## ACKNOWLEDGMENTS

The authors acknowledge the Brazilian agency CNPq for the financial support. This work is also partially supported by INCT-FCX (FAPESP-CNPq).

[1] T. F. Tadros, *Surfactants* (Academic Press, London, 1985).
[2] C. Tanford, *Hydrophobic Effect: Formation of Micelles and Biological Membranes* (Wiley, New York, 1980).
[3] R. Zana (ed.), *Dynamics of Surfactant Self-Assemblies: Micelles, Microemulsions, Vesicles and Lyotropic Phases* (CRC Press, Boca Raton, 2005).
[4] J. N. Israelachvilli, *Intermolecular and Surface Forces* (Academic Press, London, 1992).
[5] W. Gelbart, A. Ben-Shaul, and D. Roux (eds.), *Micelles, Membranes, Microemulsions, and Monolayers* (Springer, New York, 1994).
[6] D. R. Karsa, *Industrial Applications of Surfactants* (Royal Society of Chemistry, London, 1988).
[7] K. Kataoka, A. Harada, and Y. Nagasaki, Adv. Drug. Deliv. Rev. **47**, 113 (2001).
[8] J. Fendler, *Catalysis in Micellar and Macromolecular Systems* (Academic Press, New York, 1975).
[9] D. Myers, *Surfaces, Interfaces and Colloids: Principles and Applications* (VCH, New York, 1991).
[10] A. Patist, J. R. Kanicky, P. K. Shukla, and D. O. Shah, J. Colloid Interface Sci. **245**, 1 (2002).
[11] H. Wennerström and B. Lindman, Phys. Rep. **52**, 1 (1979).

[12] J. N. B. de Moraes and W. Figueiredo, J. Chem. Phys. **110**, 2264 (1999).
[13] G. Gunnarsson, B. Jönsson, and H. Wennerström, J. Phys. Chem. **84**, 3114 (1980).
[14] A. Jusufi, D. N. LeBard, B. G. Levine, and M. L. Klein, J. Phys. Chem. B **116**, 987 (2012).
[15] B. L. Bales, J. Phys. Chem. B **105**, 6798 (2001).
[16] M. Girardi and W. Figueiredo, J. Chem. Phys. **112**, 4833 (2000).
[17] H.-U. Kim and K.-H. Lim, Colloid Surf. A: Physicochem. Eng. Aspects **235**, 121 (2005).
[18] S. Paula, W. Süs, J. Tuchtenhagen, and A. Blume, J. Phys. Chem. **99**, 11742 (1995).
[19] T. M. Perger and M. Bester-Rogac, J. Colloid Interface Sci. **313**, 288 (2007).
[20] J. R. Davis and A. Z. Panagiotopoulos, J. Chem. Phys. **131**, 114901 (2009).
[21] A. Jusufi, M. L. Klein, and A. Z. Panagiotopoulos, J. Phys. Chem. B. **115**, 990 (2011).
[22] D. W. Cheong and A. Z. Panagiotopoulos, Langmuir **22**, 4076 (2006).
[23] B. Lindman and B. Brun, J. Colloid Interface Sci. **42**, 388 (1973).
[24] H. Zettl, Y. Portnoy, M. Gottlieb, and G. Krausch, J. Phys. Chem. B **109**, 13397 (2005).
[25] R. Barnadas-Rodriguez and J. Esterlich, J. Phys. Chem. B **113**, 1972 (2009).
[26] S. Niu, R. K. Gopidas, N. J. Turro, and G. Gabor, Langmuir **8**, 1271 (1992).
[27] M. Beija, A. Fedorov, M. T. Charreyre, J. M. G. Marinho, and M. G. Jose, J. Phys. Chem. B **114**, 9977 (2010).
[28] T. Sakai, Y. Kaneko, and K. Tsujii, Langmuir **22**, 2039 (2006).
[29] X. Cui, S. Mao, H. Yuan, and Y. Du, Langmuir **24**, 10771 (2008).
[30] A. D. Mackie, A. Z. Panagiotopoulos, and I. Szleifer, Langmuir **13**, 5022 (1977).
[31] R. Hadgiivanova and H. Diamant, J. Phys. Chem. B **111**, 8854 (2007).
[32] R. Hadgiivanova and H. Diamant, J. Phys. Chem. B **130**, 114901 (2009).
[33] R. Hadgiivanova, H. Diamant, and D. Andelman, J. Phys. Chem. B **115**, 7268 (2011).
[34] D. N. LeBard, B. G. Levine, R. DeVane, W. Shinoda, and M. L. Klein, Chem. Phys. Lett. **522**, 38 (2012).
[35] E. A. G. Aniansson and S. N. Wall, J. Phys. Chem. **78**, 1024 (1974).
[36] E. A. G. Aniansson, S. N. Wall, M. Almgren, H. Hoffman, I. Kielmann, W. Ulbricht, R. Zana, J. Lang, and C. Tondre, J. Phys. Chem. **80**, 905 (1976).
[37] R. G. Larson, J. Chem. Phys. **89**, 1642 (1988).
[38] R. G. Larson, J. Chem. Phys. **96**, 7904 (1992).
[39] A. Z. Panagiotopoulos, M. A. Floriano, and S. K. Kumar, Langmuir **18**, 2940 (2002).
[40] J. C. Desplat and C. M. Care, Mol. Phys. **87**, 441 (1996).
[41] C. M. Care, J. Phys. C: Solid State. Phys. **20**, 689 (1987).
[42] G. Heinzelmann, W. Figueiredo, and M. Girardi, J. Chem. Phys. **131**, 144901 (2009).
[43] J. N. B. de Moraes and W. Figueiredo, J. Phys. Chem. B **111**, 5648 (2007).
[44] M. Girardi, V. B. Henriques, and W. Figueiredo, Chem. Phys. **316**, 117 (2005).
[45] M. Girardi, V. B. Henriques, and W. Figueiredo, Chem. Phys. **328**, 139 (2006).
[46] M. Lisal, C. K. Hall, and K. E. Gubbins, J. Chem. Phys. **116**, 1171 (2002).
[47] M. Lisal, C. K. Hall, K. E. Gubbins, and A. Z. Panagiotopoulos, Fluid Phase Equilibr. **194**, 233 (2002).
[48] G. Heinzelmann, W. Figueiredo, and M. Girardi, Chem. Phys. Lett. **550**, 83 (2012).
[49] M. E. J. Newman and G. T. Barkema, *Monte Carlo Methods in Statistical Physics* (Clarendon Press, Oxford, 1998).
[50] D. P. Landau and K. Binder, *A Guide to Monte Carlo Simulations in Statistical Physics* (Cambridge University Press, Cambridge, 2000).
[51] J. N. B. de Moraes and W. Figueiredo, Chem. Phys. Lett. **491**, 39 (2010).